The 2010 IEEE/RSJ International Conference on
Intelligent Robots and Systems
October 18-22, 2010, Taipei, Taiwan

Microassembly Using a Variable View Imaging System to Overcome Small FOV and Occlusion Problems

Xiaodong Tao, Hyungsuck Cho, *Senior Member, IEEE* and Deokhwa Hong

Abstract— **In this paper, the variable view imaging system (VVIS) developed to offer flexibility in microscopic observation is applied to microassembly tasks to overcome several problems in normal imaging systems that hindered application of vision-guided micromanipulation techniques such as limited field of view (FOV) and fixed viewing direction. In three representative cases of microassembly, the parts are mated by visual servoing, avoiding FOV problem by combining unit FOV's and occlusion problem by changing the viewing direction to the optimal one. The results demonstrate the superiority and usefulness of the VVIS in various micromanipulation tasks.**

I. Introduction

OBSERVATION of dynamic targets in 3D space is drawing increasing interest as MEMS (micro-electro-mechanical system) and biotechnologies are developed [1,2]. Keeping the region of interest (ROI) on a moving target from the best view direction is critical for observation. Especially for the cases of microassembly and micromanipulation, the two-directional interaction between a micromanipulator/ microrobot and a vision system is an important factor for the success of those tasks. Unfortunately, the conventional microscopes used in most of these applications cannot meet this requirement. Insufficient vision information in these systems, such as occlusion, a small field of view (FOV) and low depth resolution often hinders the success of micro inspection, microassembly and/or micromanipulation.

In macro word, by installing a camera on a manipulator, the active vision system can change camera parameters such as the spatial position and orientation according to different tasks [3, 4]. However, mounting a microscope on a manipulator is not practical owing to the complexity of the microscope. Instead of moving vision system, moving stages are often applied in order to compensate the problem of small FOV in observation of moving objects [5, 6]. But it may generate agitation to the specimen. In order to observe different view for micro objects, multiple fixed microscope are often applied in microassembly and micromanipulation application. Stephen J. Ralis [7] proposed a microassembly system with two cameras. One camera with low magnification is to observe a wide field of view in coarse visual servoing and the other with high magnification to detect micro targets in a small field of view with high resolution in fine visual servoing. When dealing the micro object with three dimensional shapes, more cameras are needed to achieve sufficient vision information. Probst et al. [8] designed a microassembly system with three cameras in different direction. Visual guided microassembly can be applied successfully without occlusion. However, due to the fixed position of the cameras, this configuration is only suitable for specific microassembly task and switching between those cameras during microassembly makes continual visual tracking difficult. Jasper et al. [9] designed a CameraMan robot for a nanohandling system, which can move a microscope in different view angle. However the speed of the motion is limited by the weight of the microscope. The development of smart optical system with adjustable optical parameters becomes a promising solution. One example is the Adaptive Scanning Optical Microscope (ASOM) invented by Potsaid et al. [10]. Through the integration of a scanning mirror and deformable mirror, the ASOM can steer a sub-field-of-view in a large area. This system has been applied in microassembly and micro manipulation. Another example is the Wide-Angle View Endoscope System invented by Kobayashi et al. [11], which can observe a wide area without moving the endoscope.

In previous publications [12-16], an optomechatronic system that has been termed a VVIS (Variable View Imaging System) is introduced. In this paper, we show an application of the VVIS in microassembly tasks where variable view is very useful in changing the size and position of the FOV to cover varying work space and changing the viewing direction to avoid occlusions.

II. System Configuration

Fig. 1 shows the layout of the VVIS and the microassembly system attached in the object space. The view position and angles can be steered by special designed active optical component. In order to realize this function, the idea is to design the vision system with active components which mimic the function of robot. To steer the view orientation, double wedge prisms are applied which can steer the beam in any direction in a cone. This function is similar to a camera installed on a pan/tilt stage. To steer the view position, the telecentric scanner is applied, which is similar to a camera installed on the translation stage. In order to steer the both of view position and orientation, these two active optical components can be integrated into one system.

Manuscript received March 10, 2010. This work was supported in part by the Brain Korea 21 project by Korean Government.

X. Tao is with the University of California, Santa Cruz, CA 95064 USA (e-mail: jamest0101@hotmail.com).

H. S. Cho, is Chair Professor with Daegu Kyungbuk Institute of Science and Technology (DGIST), Korea (phone: +82-42-350-3213; fax: +82-42-350-3210; e-mail: hscho@kaist.ac.kr).

D. Hong is with Korea Advanced Institute of Science and Technology, Daejeon 305-701 Korea (e-mail: hdh@kaist.ac.kr).

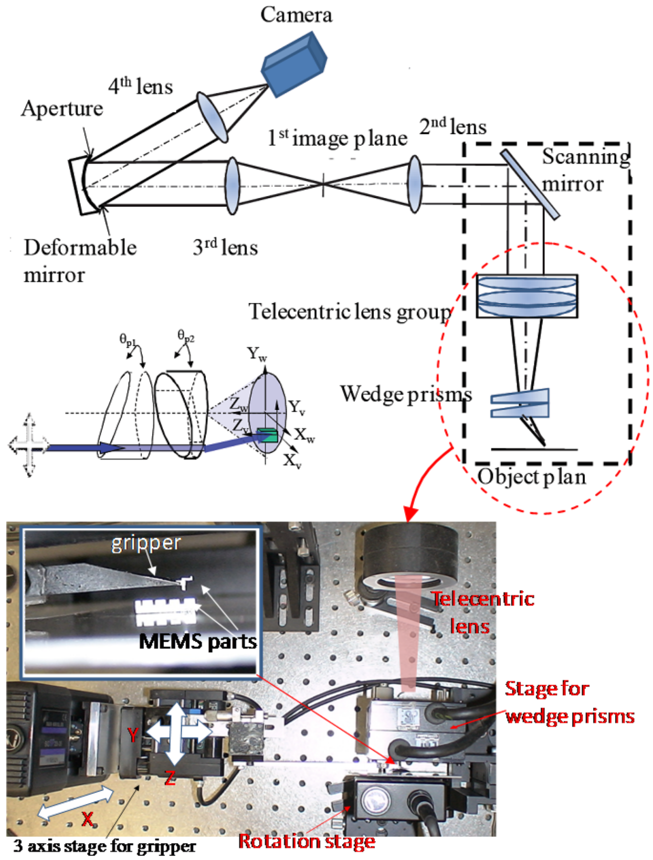

Fig. 1. Configuration of the microassembly system attached in the VVIS.

The microassembly system includes a 3DOF micromanipulator which has a repeatability of 0.1 um in Z and Y directions and 3 um in X direction. Z and Y stages are actuated by DC motors and the range is 15 mm. X stage is actuated by a step motor and the range is 35mm. Due to the shortage of ports on the computer for the VVIS, the manipulators are connected to another computer and the two computers are connected by serial port.

III. Microassembly Tasks

In this Section three microassembly tasks are presented that representatively show the necessity of the VVIS in assembly process. Those tasks are shown in Fig. , and the dimension of each object is shown in Fig. 3.

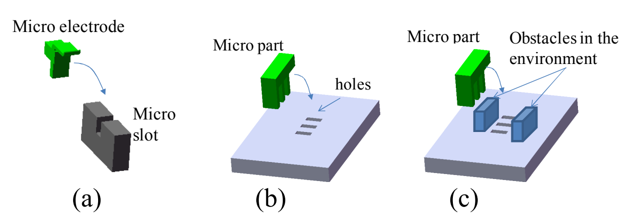

Fig. 2. MEMS Microassembly tasks: (a) Task1: micro part with a single leg (b) Task2 : micro part with multi-legs (c) Task3 : micro part with obstacles.

The first task is mating a micro part with a single leg and a micro slot that are initially located 6mm apart each other as shown in Fig. 2 (a), and the second task is to insert multi-legs into multi-holes as shown in Fig. 2 (b). The third task is to insert the multi-legged part to the multi-holes having other objects around them which cause severe occlusion as shown in Fig. 2 (c). For those tasks, vision-guided assembly task cannot be performed successfully using fixed vision systems due to small FOV and occlusion issues as represented in the exemplary case shown in Fig. 4. In that, the image features (C_1, C_2) are occluded by the parts (Fig. 4 (a)) or they are not obtained in one image due to their initial distance (Fig. 4 (b)). These problems can be solved by introducing the VVIS to change the viewing direction or extending the FOV. The third task shows more complicated situation that not only those parts to be assembled but also other obstacles also occludes the image features. In that case finding the best viewing direction to avoid the occlusion problem is important as shown in Fig. 5 and this may not be found if the viewing angle is not adjustable.

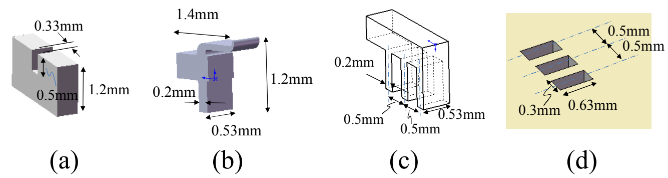

Fig. 3. Dimension of micro parts: (a) micro slot (b) micro electrode (c) micro part with multi legs (d) micro holes.

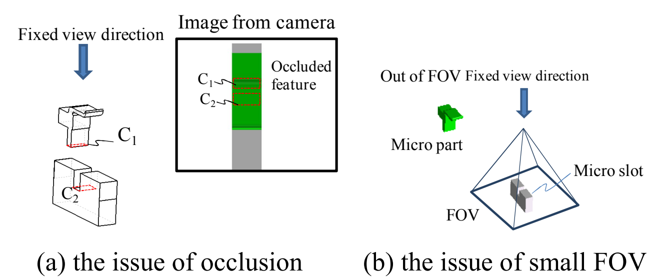

Fig. 4. Issues for the 1st task when using a conventional optical system: (a) occlusion and (b) small FOV.

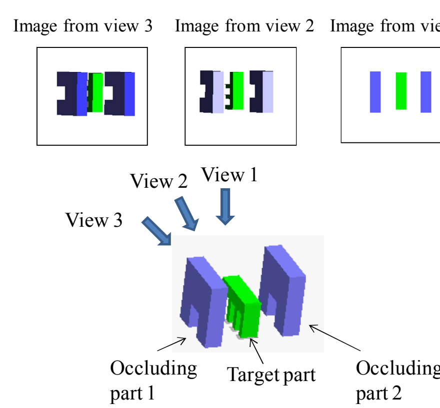

Fig. 5. Images from different views in the third experiment.

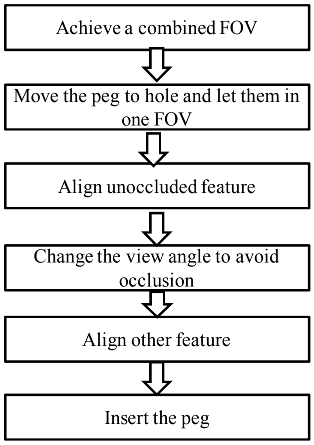

Fig. 6. Microassembly process.

IV. PROCESS FOR THE VISION GUIDED MICROASSEMBLY

The microassembly tasks introduced in the previous section are peg-in-hole task. The goal of those tasks is to align the features on pegs to the corresponding ones of the holes and to insert them. However, because of small FOV and occlusion during assembly, the operation of the optical system should be considered to supply sufficient vision information during the microassembly. The assembly strategy using the VVIS is shown in Fig. 6. First, a combined FOV can be achieved by moving the FOV, which covers both targets. Then the peg is moved to the hole so that both targets are in one FOV. The third step is to align the unoccluded features on peg and hole. The fourth step is to change the view direction to observe the occluded feature. Then these features are aligned in the fifth step. The final step is to insert the peg into the hole.

In aligning steps (third and fifth), corner features are extracted to calculate the error between the current position and the desired one. For the ith feature point, $(u_i, v_i)^T$, and its corresponding destination, $(u_{di}, v_{di})^T$, position error vector can be defined as follows:

$$\mathbf{e} = \left(\mathbf{e}_1^{\mathrm{T}} \quad \cdots \quad \mathbf{e}_i^{\mathrm{T}} \quad \cdots \quad \mathbf{e}_n^{\mathrm{T}}\right)^{\mathrm{T}}, \quad \mathbf{e}_i = \begin{pmatrix} u_{di} - u_i \\ v_{di} - v_i \end{pmatrix} \tag{1}$$

where n is the number of the feature points.

Then, the velocity command for the gripper can be obtained as follows:

$$\begin{bmatrix} V_x \\ V_y \end{bmatrix} = kJ^{\dagger}\mathbf{e} \tag{2}$$

where k is gain factor and J is the image Jacobian defined as

$$J = \left(J_1^{\mathrm{T}} \quad \cdots \quad J_i^{\mathrm{T}} \quad \cdots \quad J_n^{\mathrm{T}}\right)^{\mathrm{T}}, \quad J_i = \begin{bmatrix} Km & 0 \\ 0 & Km \end{bmatrix} \tag{3}$$

where K is a camera scaling factor and m is the magnification of the system. The feedback gain k can be adjusted case by case.

For the first task, the whole process is considered, but in the second and third tasks, we assume the peg and hole are already close enough to be inside of one FOV.

A. Assembly process for Task1

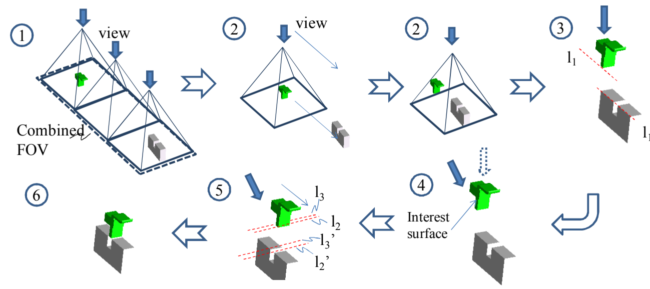

Fig. 7. Process for the first microassembly task.

The whole process of the first task is shown in Fig. 7. In step1, a combined FOV is obtained which can cover both the micro electrode and the micro slot as shown in Fig.8. Then the corner feature is captured by Harris Conner detector as shown in Fig.8, where p_1, p_2, p_3 and p_4 are corners on the electrode and p_1', p_2', p_3' and p_4' on the slot. In step2, the electrode moves towards to the slot. Visual servoing is applied here to guide the feature point p_3 on the electrode to a desired point p_d which is near to the micro slot. The velocity command for the gripper is calculated using (2).

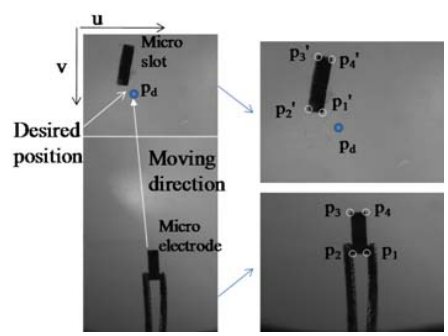

Fig.8. The combined FOV and definition of corner points.

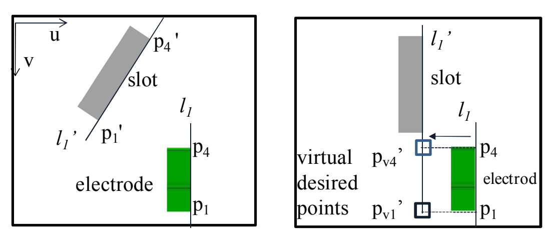

(a) (b)

Fig. 9. Alignment of line l_1 with l_1', (a) removing the angular error (b) removing the position error.

In step3, the unoccluded feature line l_1 and l_1' are aligned as shown in Fig.9. In order to remove the angular error, the command for rotation stage is defined as follows,

$$[\omega_z] = k_\omega \left(\tan^{-1}\left(\frac{v_{p1} - v_{p4}}{u_{p1} - u_{p4}} \right) - \tan^{-1}\left(\frac{v_{p1}' - v_{p4}'}{u_{p1}' - u_{p4}'} \right) \right) \qquad (4)$$

where k_ω is the gain factor. In order to remove the position error, virtual desired points are defined as an intersection point between l_1' and the normal of the line l_1' from p_1 and p_3. In step4, a view to avoid occlusion is obtained by the VVIS for the interest surface.

In step5, the feature lines l_3, l_2 are aligned with the feature lines l_3' and l_2' as shown in Fig. 20. The lines l_2' and l_3' are obtained by detecting the corners on the line. Then the center line l_{23}' between l_2',l_3' is obtained. The point P_{56} is the center point between the corner point P_5 and P_6. Then the virtual desired points P_{v23}' is obtained by the intersection between the normal of l_{23}' through p_{56} and the line l_{23}'. In this step, the point P_{56} moves to the virtual desired point P_{v23}'. The command for the gripper is calculated using (2).

In step6, the micro electrode is inserted into the slot as illustrated in Fig. 31. The center point p_{56} between the corner point p_5, p_6 on the electrode moves to the center point p_{56}' between the corner point p_5' and p_6'. The command for the gripper is defined as

$$V_z = k_4 \left\| p_{56}' - p_{56} \right\| \qquad (5)$$

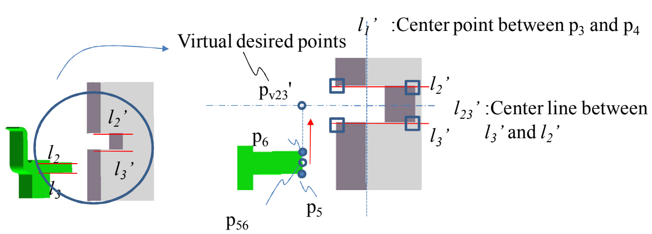

Fig. 20. Alignment of line l_2, l_3 with l_2',l_3'.

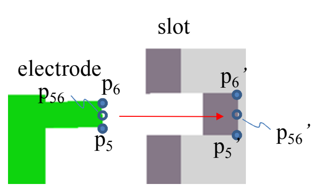

Fig. 31. Inserting the micro part.

B. *Assembly process for Task2*

In the second task, we assume the objects are in inside of one FOV, and the angular error between the two parts has been removed. Therefore, only the last four steps in Fig. are considered. The overall process is shown in Fig. 42. The first two steps are similar to those in the first task. In step3, the virtual points p_{23}', p_{45}', p_{67}' are the perpendicular foots of points p_{23}, p_{45} and p_{67} to the line l_{23}', l_{45}', l_{67}' as depicted in Fig. 53. Line l_{23}' is the center line of l_2'and l_3'. L_{45}' is the center line of l_4' and l_5'. L_{67}' is the center line of l_6' and l_7'. In this step, the points p_{23}, p_{45} and p_{67} moves to the virtual desired points p_{23}', p_{45}', p_{67}'. The command for the gripper is obtained by (2). In step4, the micro part is inserted to the micro hole. The virtual points p_{h23}', p_{h45}' and p_{h67}' on the hole are the center points between two corner of holes as depicted in Fig. 64. The goal is to move the points p_{23}, p_{45} and p_{67} to the virtual points p_{h23}', p_{h45}' and p_{h67}', which will guide the micro part into the micro hole. The command for the gripper is defined as follows,

$$V_z = k_6 \left(\min\left(\left\| p_{23}' - p_{23} \right\| + \left\| p_{45}' - p_{45} \right\| + \left\| p_{67}' - p_{67} \right\| \right) - T \right) \qquad (6)$$

where k_6 is the gain factor, T is a safety threshold, which is defined as 20 pixels to avoid collision between two parts.

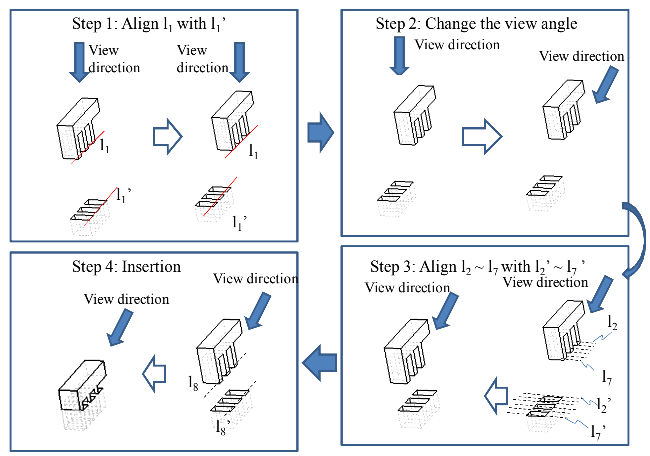

Fig. 42. Process for the third microassembly task.

C. *Assembly process for Task3*

For the third task, the process is almost similar to the second one but some peripheral obstacles that occlude the surface of interest in step 3. The interest surface and configuration of the micro parts are shown in Fig. 5. The view planning method proposed in [7] is applied here. In this method, the best view angle is calculated by maximize the resolution of the interest surface under acceptable occlusion level. The view position is steered by visual feedback method which can keep the target inside of field of view.

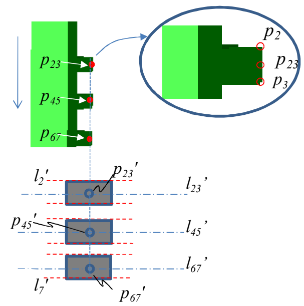

Fig. 53. Step3 in the second task.

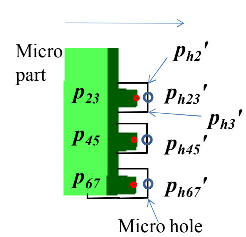

Fig. 64. Step4 in the second task.

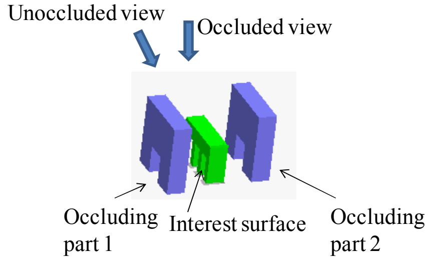

Fig. 15. Configuration of micro parts in Task 3.

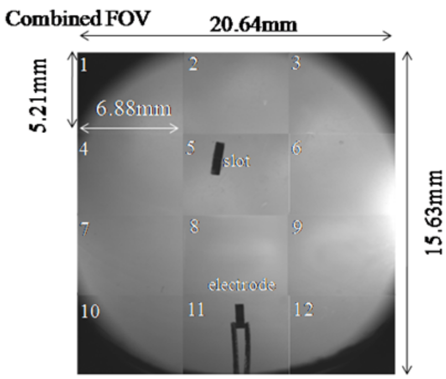

Fig. 76. Image of the combined FOV.

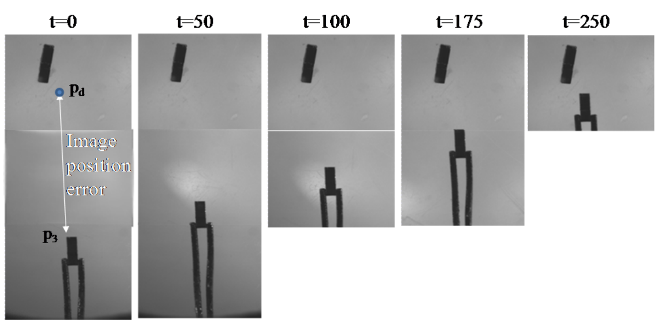

Fig. 87. Snapshots during step1.

V. Experimental Results

A. Task1

In step1, in order to detect the object in a big work space, a combined FOV is obtained as shown in Fig. 76. The combined FOV includes 12 unit FOVs, of which the dimension is 5.21×6.88mm^2. The dimension of combined FOV is 15.63mm×20.64mm. The resolution of each view is 10 um. As can be seen, a large FOV with high resolution can be obtained using the VVIS. During step2, the micro electrode is moved towards the slot. Some snapshots are shown in Fig. 87. As can be seen, initially 3 unit FOVs were combined and after 50 iterations, the combined FOV only consist of 2 unit FOVs. In the final state, only one view is needed. During step3, the angular and position errors between the parts are removed by visual servoing. In step4, the best view angle is calculated using the potential field method [7]. Their corresponding images are shown in Fig.19. As can be seen from the image, the occluded surface can be observed in the view generated by the proposed system. In step5, the peg and the slot are again aligned. Some snapshots are shown in Fig. 20. As can be seen, the occluded featured can be observed and aligned using the VVIS. The final step is to insert the electrode into the slot. Some snapshots are shown in Fig.0. As can be seen from the image, the image error converges to 0 after 300 iterations. The final image shows the success of the microassembly.

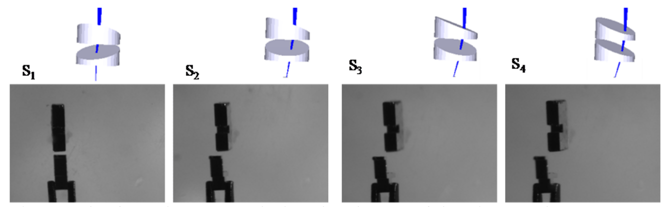

Fig.18. The four view states during the change of the view angle.

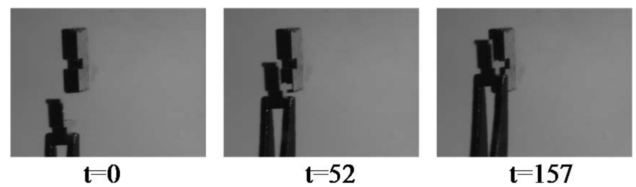

Fig. 19. Snapshots during alignment in the step5 of the first task.

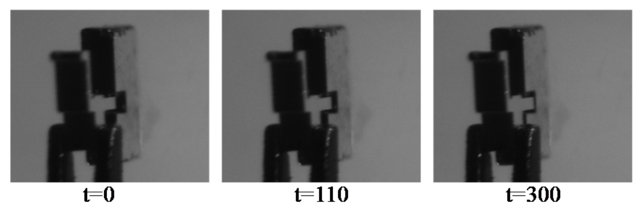

Fig.20. Snapshots of the step6 of the first task.

B. Task2

The second task is assembly of a multi-legged part and multi slots. The aligning methods are explained in the previous section and basically the same as that of the first task. After that, view direction is changed to avoid occlusions. As in the case of Task1, potential field is generated according to the view planning method [7]. Some snapshots of view direction change and their corresponding prism configurations are shown in Fig. 91. In the step3, the image features of each part are again aligned, and some snapshots are shown in Fig. 102. The image error is converged to 0 after 210 iterations. Then the legged part is inserted into the hole, as shown in Fig. 113.

C. Task3

In the third task, most of the assembly process is same as the second one but step2, the occlusion avoidance. The interested surface is occluded by other two objects as shown in Fig. 124. In order to avoid that occlusion, the view planning method [7] was applied, and Fig.25 shows some view states during the view change. As shown in the last image, the micro hole can be observed without occlusion. Because the micro holes are visible, the legged part can be aligned and inserted into the holes in the same way as Task2.

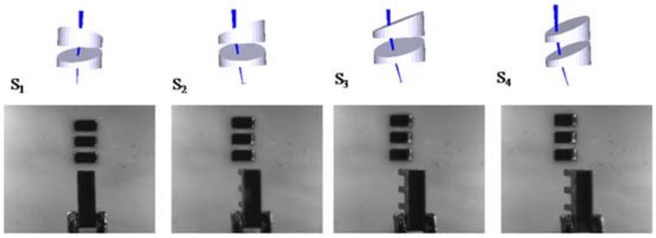

Fig. 91. Snapshots during the view change in the second task.

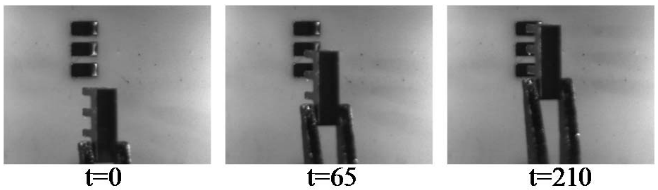

Fig. 102. Snapshots during assembly in the step 3 of the second task..

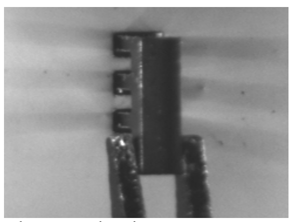
Fig. 113.Final state in the second task..

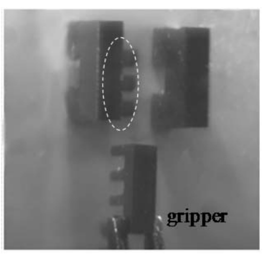

Fig. 124. The occlusion in the third task.

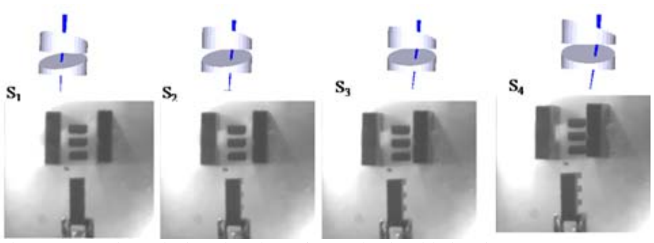

Fig.25. Snapshots during the view change in the third task

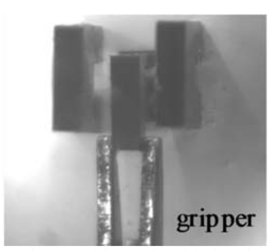

Fig.26. The final image of assembly in the third task.

VI. CONCLUSION

In this paper, we demonstrated the feasibility of applying VVIS in microassembly tasks which otherwise cannot be performed successfully due to limited FOV and occlusion problems through three representative cases. The small FOV problem could be handled by stitching unit FOVs, and occlusion problem could be solved by changing the view direction. The experimental results show that the VVIS is very useful in vision-guided micromanipulation tasks owing to its flexibility. Full automation of the process is left as a future work.

REFERENCES

[1] A. Georgiev, P. K. Allen, W. Edstrom, “Visually-guided protein crystal manipulation using micromachined silicon tools,” IEEE/RSJ International Conference on Intelligent Robots and Systems, 2004

[2] S. Ralis, B. J. Nelson, B. Vikramaditya, "Micropositioning of a Weakly Calibrated Microassembly System Using Coarse-To-Fine Visual Servoing Strategies", IEEE Transactions on Electronic Packaging Manufacturing, Vol. 23, No. 2, pp. 123 – 131, April 2000.

[3] Y. Mezouar, and F. Chaumette, “Avoiding self-occlusions and preserving visibility by path planning in the image”, Robotics and Autonomous Systems, Vol 41, Issues 2-3, 77-87, 30 November 2002,

[4] B. Nelson and P.K. Khosla, "The Resolvability Ellipsoid for Sensor Based Manipulation," CMU-RI-TR-93-28, The Robotics Institute, Carnegie Mellon University

[5] H. Xie, L. N. Sun, W. B. Rong, "A flexible experimental system for complex microassembly under microscale force and vision-based control," Int. J. Optomechatron.. 1, 81-101, 2007.

[6] N. Ogawa, H. Oku, K. Hashimoto, and M. Ishikawa, "Microrobotic visual control of motile cells using high-speed tracking system", IEEE Trans. Robotics, vol. 21, no. 3, Jun. 2005

[7] S. J. Ralis, B. Vikaramadiya, B. J. Nelson, "Micropositioning of a Weakly Calibrated Microassembly System Using Coarseto-Fine Visual Servoing Strategies, " IEEE Transactions on Electronics Packaging Manufactureing , Vol 23, No. 2, pp. 123-131, 2000

[8] M. Probst, K. Vollmers, B. E. Kratochvil, B. J. Nelson, "Design of an Advanced Microassembly System for the Automated Assembly of Bio-Microrobots", Proc. 5th International Workshop on Microfactories, 2006.

[9] D.Jasper, C.Dahmen, S.Fatikow: "CameraMan - Robot Cell with Flexible Vision Feedback for Automated Nanohandling inside SEMs", IEEE Conference on Automation Science and Engineering (CASE 2007), Scottsdale, USA, September 22-25, pp.51-56, 2007

[10] B. Potsaid, Y. Bellouard, and J. Wen, “Adaptive Scanning Optical Microscope (ASOM): a multidisciplinary optical microscope design for large field of view and high resolution imaging,” Opt. Express 13(17), 6504–6518, 2005

[11] E. Kobayashi, K. Masamune, I. Sakuma, T. Dohi: A Wide-Angle viewEndoscope System Using Wedge Prisms, MICCAI 2000, p.661-668, 2000

[12] X. Tao, H. Cho, and F. Janabi-Sharifi, “Active optical system for variable view imaging of micro objects with emphasis on kinematic analysis, ”Appl. Opt., 47(22), 4121-4132, 2008

[13] X. Tao and H. Cho, “Variable View Imaging System: An Optomechatronic System for the Observation of Micro Objects with Variable View Direction”, International Journal of Optomechatronics,Volume 3, Issue 2,pp. 91-115,2009.

[14] X. Tao , D. Hong, and H. Cho, “Variable view imaging system with decoupling design,” International Symposium on Optomechatronic Technologies, Proc. of SPIE,Vol. 7266,pp. 72661U-1 - 11,2008.

[15] X. Tao, H. Cho, and F. Janabi-Sharifi, “Optical design of a variable view imaging system with the combination of a telecentric scanner and double wedge prisms”, APPLIED OPTICS, Vol. 49, No. 2, pp.239-246, 2010

[16] X. Tao, H. Cho and K. C. Koh, “View Planning to Increase the Visibility for Observing Micro Objects using a Variable View Imaging System”, ISOT 2009, September, Turkey, pp. 299-304, 2009.